

Small Signal Modeling of LLC Resonant Converters Based on Extended Describing Function

Chien-Hsuan Chang, En-Chih Chang, Chun-An Cheng, Hung-Liang Cheng and Sheng-Chang Lin
 Department of Electrical Engineering,
 I-Shou University,
 Kaohsiung 84001, Taiwan
 e-mail: chchang@isu.edu.tw

Abstract—Due to the advantages of low switching loss and high efficiency, LLC resonant converters have been widely used. Based on the extended describing function concept, the small-signal model of an LLC resonant converter is derived in this paper. The equivalent circuit of small-signal model is illustrated so that the corresponding frequency response can be easily obtained by using IsSpice simulation. The well agreement with experimental measurements has verified the accuracy of the derived small-signal model.

Keywords- LLC Resonant Converter; Small Signal Model; Extended Describing Function

I. INTRODUCTION

The power switches of traditional pulse-width-modulation (PWM) dc-dc converters operate in hard switching, which results in high switching loss and electromagnetic interference issues. Numerous resonant converters [1]-[4], such as series resonant converter (SRC) [1], parallel resonant converter (PRC) [1], series-parallel resonant converter (SPRC) [2], [3], and LLC resonant converter [4] are proposed to solve these problems.

SRC provides satisfied efficiency, but it has the problem of output voltage regulation at light load condition. Although PRC has no light load regulation issue, its circulating energy is much higher than SRC and impacts efficiency significantly. SPRC remains the advantages of SRC and PRC, which are smaller circulating energy and not so sensitive to load change. However, the same as SRC and PRC, SPRC requires operating at very high switching frequency to obtain extremely low output voltage. Therefore, with low output voltage operation, all of SRC, PRC, and SPRC possess high circulating energy to lower their efficiencies [4].

At high input voltage or low output voltage operation, the LLC resonant converter has smaller circulating energy than SRC, PRC and SPRC. Both the active switches of an LLC resonant converter can turn on with zero voltage switching (ZVS), and both the output rectifier diodes can turn off with zero current switching (ZCS), which can result in higher conversion efficiency. Therefore, LLC resonant converters have been widely used in the high power or high frequency applications.

The state space average method [5] is the most popular approach for modeling PWM converters. It provides simple and accurate solution for up to half the switching frequency. Unfortunately, since the natural frequency of a resonant converter is close to its switching frequency, this method cannot be applied for modeling. The sample-data modeling approach was proposed in [6] as a systematic method for modeling resonant converters. However, it is solved in the numerical form and is difficult to apply for the compensator design. A small-signal modeling approach based on extended describing function (EDF) [7] concept has been applied to SRC, PRC and SPRC [1], [3].

This paper will derive the small-signal model of an LLC resonant converter based on the EDF concept. The corresponding Bode plots can be easily obtained from IsSpice simulation of the equivalent circuit model. The accuracy of the derived model can be verified by comparing with experimental results. This simple analytical model is beneficial for the feedback compensator design of an LLC resonant converter.

II. SMALL-SIGNAL MODELING

Fig. 1 shows the schematic diagram of an LLC resonant converter. In this section, the modeling procedure will be addressed step by step. For simplifying the derivation, following conditions are made:

- 1) The amplitude of perturbation signal is very small, and its frequency is much lower than switching frequency.
- 2) The waveforms of resonant components will be regarded as sinusoidal.
- 3) All switching components are ideal.

A. Nonlinear State Equation

According to the circuit shown in Fig. 1, while power switches S_1 and S_2 are conducting alternately, a symmetrical square waveform, v_{ab} can be obtained. Its magnitude, V_g should be half the input voltage. Fig. 2 shows the equivalent circuit of an LLC resonant converter, in which C_o is equivalent output capacitance, r is the equivalent ESR, and R_l is equivalent load resistance seen in primary side. According to this equivalent circuit, the nonlinear state equations are given by:

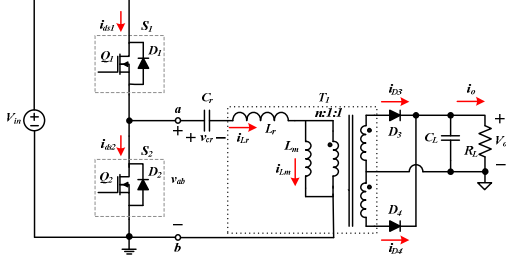


Figure 1. Schematic diagram of an LLC resonant converter.

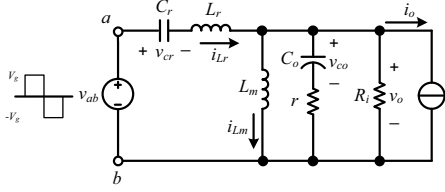


Figure 2. Equivalent circuit of an LLC resonant converter.

$$L_r \frac{di_{Lr}}{dt} + v_{Cr} + L_m \frac{di_{Lm}}{dt} = v_{ab} \quad (1a)$$

$$L_m \frac{di_{Lm}}{dt} = \text{sgn}(i_{Lr} - i_{Lm}) \cdot v_o \quad (1b)$$

$$C_r \frac{dv_{Cr}}{dt} = i_{Lr} \quad (1c)$$

$$\left(1 + \frac{r}{R}\right) C_o \frac{dv_{co}}{dt} + \frac{1}{R_i} v_{co} = |i_{Lr} - i_{Lm}| + i_o \quad (1d)$$

$$v_o = \frac{r \cdot R_i}{r + R_i} (|i_{Lr} - i_{Lm}| + i_o) + \frac{R_i}{R_i + r} \cdot v_{co} \quad (1e)$$

$$i_g = \frac{1}{T} \int_0^T i_{Lr} \frac{v_{ab}(t)}{v_g} dt \quad (1f)$$

where i_{Lr} , i_{Lm} , v_{Cr} , v_{co} are state variables, and v_o , i_g are output variables. In the LLC resonant converter, the output voltage can be regulated by modulating switching frequency, ω_s or duty cycle, d . The operation point is determined by $\{v_g, i_o, R_i, \omega_s, d\}$.

B. Harmonic Approximation

While the LLC resonant converter is operating in steady state, the waveforms of resonant components are nearly sinusoidal. The resonant currents i_{Lr} , i_{Lm} , and the resonant voltage v_{Cr} , can be approximated by fundamental harmonics as following:

$$i_{Lr} \approx i_{Lrs}(t) \sin \omega_s t + i_{Lrc}(t) \cos \omega_s t \quad (2a)$$

$$i_{Lm} \approx i_{Lms}(t) \sin \omega_s t + i_{Lmc}(t) \cos \omega_s t \quad (2b)$$

$$v_{Cr} \approx v_{Crs}(t) \sin \omega_s t + v_{Crc}(t) \cos \omega_s t \quad (2c)$$

The derivatives of i_{Lr} , i_{Lm} , and v_{Cr} are given by:

$$\frac{di_{Lr}}{dt} = \left(\frac{di_{Lrs}}{dt} - \omega_s i_{Lrc}\right) \sin \omega_s t + \left(\frac{di_{Lrc}}{dt} + \omega_s i_{Lrs}\right) \cos \omega_s t \quad (3a)$$

$$\frac{di_{Lm}}{dt} = \left(\frac{di_{Lms}}{dt} - \omega_s i_{Lmc}\right) \sin \omega_s t + \left(\frac{di_{Lmc}}{dt} + \omega_s i_{Lms}\right) \cos \omega_s t \quad (3b)$$

$$\frac{dv_{Cr}}{dt} = \left(\frac{dv_{Crs}}{dt} - \omega_s v_{Crc}\right) \sin \omega_s t + \left(\frac{dv_{Crc}}{dt} + \omega_s v_{Crs}\right) \cos \omega_s t \quad (3c)$$

C. Extended Describing Function

The nonlinear terms (v_{ab} , $\text{sgn}(i_{Lr} - i_{Lm})$, $|i_{Lr} - i_{Lm}|$, i_g) in (1) can be approximated either by the fundamental components or by the dc components:

$$v_{ab} \approx f_1(v_g, d) \sin \omega_s t \quad (4a)$$

$$\text{sgn}(i_{Lr} - i_{Lm}) \cdot v_o \approx f_2(i_{Lrs} - i_{Lms}, v_{co}) \sin \omega_s t + f_3(i_{Lrc} - i_{Lmc}, v_{co}) \cos \omega_s t \quad (4b)$$

$$|i_{Lr} - i_{Lm}| \approx f_4(i_{Lrs} - i_{Lms}, i_{Lrc} - i_{Lmc}) \quad (4c)$$

$$i_g \approx f_5(i_{Lrs}, d) \quad (4d)$$

These $f_k(*, *)$ in (4) are called extended describing functions (EDFs) [7]. By applying Fourier expansions for the nonlinear terms, their corresponding EDFs can be obtained as following:

$$f_1(v_g, d) = \frac{4}{\pi} \cdot \sin(\pi \cdot d) \cdot v_g \quad (5a)$$

$$f_2(i_{Lrs} - i_{Lms}, v_{co}) = \frac{4}{\pi} \cdot \frac{i_{Lrs} - i_{Lms}}{i_p} \cdot v_{co} \quad (5b)$$

$$f_3(i_{Lrc} - i_{Lmc}, v_{co}) = \frac{4}{\pi} \cdot \frac{i_{Lrc} - i_{Lmc}}{i_p} \cdot v_{co} \quad (5c)$$

$$f_4(i_{Lrs} - i_{Lms}, i_{Lrc} - i_{Lmc}) = \frac{2}{\pi} \cdot i_p \quad (5d)$$

$$f_5(i_{Lrs}, d) = \frac{2}{\pi} \cdot i_{Lrs} \cdot \sin(\pi \cdot d) \quad (5e)$$

where

$$i_p = \sqrt{(i_{Lrs} - i_{Lms})^2 + (i_{Lrc} - i_{Lmc})^2} \quad (5f)$$

D. Harmonic Balance

Because the frequency of small-signal perturbation is much lower than the switching frequency, the converter can be regarded as steady-state operation. By substituting (2)–(5) into (1) and equating the coefficients of dc, sine, and cosine terms, following equations can be obtained:

$$L_r \left(\frac{di_{Lrs}}{dt} - \omega_s i_{Lrc} \right) + v_{Crs} + L_m \left(\frac{di_{Lms}}{dt} - \omega_s i_{Lmc} \right) = \frac{4}{\pi} \cdot \sin(\pi \cdot d) v_g \quad (6a)$$

$$L_r \left(\frac{di_{Lrc}}{dt} + \omega_s i_{Lrs} \right) + v_{Crc} + L_m \left(\frac{di_{Lmc}}{dt} + \omega_s i_{Lms} \right) = 0 \quad (6b)$$

$$L_m \left(\frac{di_{Lms}}{dt} - \omega_s i_{Lmc} \right) = \frac{4}{\pi} \cdot \frac{i_{Lrs} - i_{Lms}}{i_p} \cdot v_{co} \quad (6c)$$

$$L_m \left(\frac{di_{Lmc}}{dt} + \omega_s i_{Lms} \right) = \frac{4}{\pi} \cdot \frac{i_{Lrc} - i_{Lmc}}{i_p} \cdot v_{co} \quad (6d)$$

$$C_r \left(\frac{dv_{Crc}}{dt} - \omega_s v_{Crc} \right) = i_{Lrs} \quad (6e)$$

$$C_r \left(\frac{dv_{Crc}}{dt} - \omega_s v_{Crc} \right) = i_{Lrc} \quad (6f)$$

$$\left(1 + \frac{r}{R_i} \right) \cdot C_o \frac{dv_{co}}{dt} + \frac{1}{R_i} v_{co} = \frac{2}{\pi} i_p + i_o \quad (6g)$$

$$v_o = \frac{r \cdot R_i}{r + R_i} \left(\frac{2}{\pi} i_p + i_o \right) + \frac{R_i}{R_i + r} \cdot v_{co} \quad (6h)$$

$$i_g = \frac{2}{\pi} \cdot i_{Lrs} \sin(\pi \cdot d) \quad (6i)$$

E. Steady-State Solution

While the LLC resonant converter is operating in steady state, the state variables in (6) are constant so that their derivatives should be zero. By giving a operating point with $\{V_g, I_o, R_i, \Omega_s, D\}$, the steady-state solution can be obtained. Assuming the converter has no loss and the duty ratio, D is 0.5, the voltage transfer function of frequency control is given by:

$$M(f_s) = \frac{\left| \frac{V_o}{V_{in}} \right|}{1} = \frac{1}{2n \cdot \sqrt{(1+A)^2 \left(1 - \left(\frac{f_L}{f_s} \right)^2 \right)^2 + \frac{1}{Q_L^2} \left(\frac{f_s}{f_L} \frac{A}{1+A} - \frac{f_L}{f_s} \right)^2}} \quad (7)$$

where the inductor ratio, A , the main resonant frequency, f_H , the second resonant frequency, f_L , and the load quality factor, Q_L are defined as following:

$$A = L_r / L_m \quad (8a)$$

$$f_H = \frac{\omega_H}{2\pi} = \frac{1}{2\pi \sqrt{L_r \cdot C_r}} \quad (8b)$$

$$f_L = \frac{\omega_L}{2\pi} = \frac{1}{2\pi \sqrt{(L_r + L_m) \cdot C_r}} \quad (8c)$$

$$Q_L = R_i \times \sqrt{\frac{C_r}{L_r + L_m}} = R_i \cdot 2\pi f_L \cdot C_r \quad (8d)$$

F. Perturbation and Linearization

By substituting $v_g = V_g + \hat{v}_g$, $i_o = 0 + \hat{i}_o$, $d = D + \hat{d}$, $\omega_s = \Omega_s + \hat{\omega}_s$ into (6), and by making linearization under the small-signal assumption, the following small-signal model can be obtained:

$$L_r \frac{d\hat{i}_{Lrs}}{dt} = (\Omega_s L_r) \cdot \hat{i}_{Lrc} + E_{1s} \cdot \hat{f}_s - \hat{v}_{Crs} - L_m \frac{d\hat{i}_{Lms}}{dt} + (\Omega_s L_m) \cdot \hat{i}_{Lmc} + E_{2s} \cdot \hat{f}_s + E_d \cdot \hat{d} + K_v \cdot \hat{v}_g \quad (9a)$$

$$L_r \frac{d\hat{i}_{Lrc}}{dt} = -(\Omega_s L_r) \cdot \hat{i}_{Lrs} - E_{1c} \cdot \hat{f}_s - \hat{v}_{Crs} - L_m \frac{d\hat{i}_{Lmc}}{dt} - (\Omega_s L_m) \cdot \hat{i}_{Lms} - E_{2c} \cdot \hat{f}_s \quad (9b)$$

$$L_m \frac{d\hat{i}_{Lms}}{dt} = (\Omega_s L_m) \cdot \hat{i}_{Lmc} + E_{2s} \cdot \hat{f}_s + 2K_s \cdot \hat{v}_o + g_{pis} (\hat{i}_{Lrs} - \hat{i}_{Lms}) - g_{ps} (\hat{i}_{Lrc} - \hat{i}_{Lmc}) \quad (9c)$$

$$L_m \frac{d\hat{i}_{Lmc}}{dt} = -(\Omega_s L_m) \cdot \hat{i}_{Lms} - E_{2c} \cdot \hat{f}_s + 2K_c \cdot \hat{v}_o + g_{pic} (\hat{i}_{Lrc} - \hat{i}_{Lmc}) - g_{pc} (\hat{i}_{Lrs} - \hat{i}_{Lms}) \quad (9d)$$

$$C_r \frac{d\hat{v}_{Crc}}{dt} = \hat{i}_{Lrs} + G_s \cdot \hat{v}_{Crc} + J_{1s} \cdot \hat{f}_s = \hat{i}_{Lrs} + J_s \quad (9e)$$

$$C_r \frac{d\hat{v}_{Crc}}{dt} = \hat{i}_{Lrc} - G_s \cdot \hat{v}_{Crc} - J_{1c} \cdot \hat{f}_s = \hat{i}_{Lrc} - J_c \quad (9f)$$

$$C_o \frac{d\hat{v}_{co}}{dt} = \left(\frac{R_i}{R_i + r} \right) \cdot \left[K_s (\hat{i}_{Lrs} - \hat{i}_{Lms}) + K_c (\hat{i}_{Lrc} - \hat{i}_{Lmc}) - \frac{1}{R_i} \hat{v}_{co} + \hat{i}_o \right] \quad (9g)$$

where the variables $\{\hat{v}_g, \hat{f}_s, \hat{d}, \hat{i}_o\}$ are called the small-signal perturbations of input voltage, switching frequency, duty ratio and output current, respectively. The small-signal model of the output rectifier circuit is expressed as:

$$\hat{v}_o = \left(\frac{R_i \cdot r}{R_i + r} \right) \cdot \left[K_s (\hat{i}_{Lrs} - \hat{i}_{Lms}) + K_c (\hat{i}_{Lrc} - \hat{i}_{Lmc}) + \hat{i}_o \right] + \frac{R_i}{R_i + r} \hat{v}_{co} \quad (9h)$$

$$\hat{i}_g = \frac{2}{\pi} \cdot \hat{i}_{Lrs} \sin(\pi \cdot d) \quad (9i)$$

G. Equivalent Circuit Model

Since (9) is a linear state equation, the corresponding equivalent circuit of small-signal model can be illustrated as shown in Fig. 3. The left part of this circuit is the part of resonant tank, which is the realization of (9a) ~ (9g). Similarly, the right part is the part of output rectifier and is realized from (9h) and (9i). The equivalent circuit contains several dependent voltage and current sources. They are

controlled by the sine and cosine components of the resonant current, i_{Lr} and the magnetic current, i_{Lm} . Based on this circuit model, the Bode plot can be easily obtained from circuit simulation program, such as IsSpice. Notice that the parameters are defined in the appendix to simplify the drawing.

III. SIMULATED AND EXPERIMENTAL RESULTS

To verify the accuracy of the derived small-signal model, an LLC resonant converter with the following component parameters was built for experimental measurements:

$$\begin{aligned} L_r &= 650 \mu\text{H}, & L_m &= 1.3 \text{ mH}, & C_r &= 3.9 \text{ nF}, \\ n &= 14, & C_o &= 2200 \mu\text{F}, & r &= 60 \text{ m}\Omega, \\ R_L &= 2.83 \Omega, & f_H &= 100 \text{ kHz}. \end{aligned}$$

By applying parameters above into the small-signal circuit model shown in Fig. 3, an IsSpice simulated Bode plot of frequency-to-output transfer function is illustrated in Fig. 4(a). Fig. 4(b) shows the experimental result which is measured by a phase analyzer. Fig. 4(a) has well agreement with Fig. 4(b), which verifies the feasibility and validity of modeling an LLC resonant converter based on EDF concept.

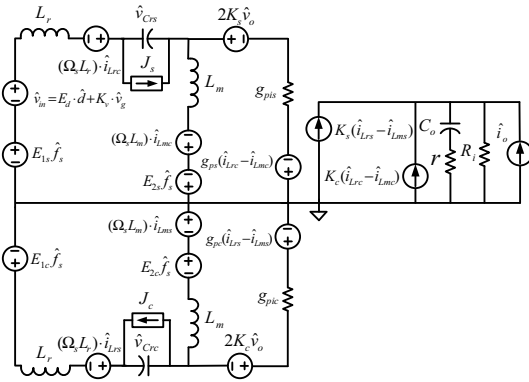


Figure 3. Equivalent circuit of the derived small-signal model.

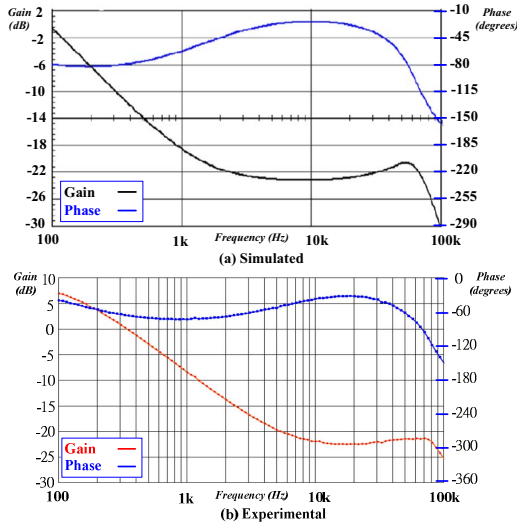


Figure 4. (a) Simulated, and (b) experimental Bode plots of frequency-to-output transfer function.

IV. CONCLUSION

The small-signal model of an LLC resonant converter is derived based on EDF concept in this paper. The equivalent circuit model is illustrated so that the corresponding Bode plot can be easily obtained by using IsSpice simulation. The well agreement with experimental measurements has verified the accuracy of the derived small-signal model. The accuracy of this model is not restricted to the operating conditions with high load quality factor. The simple analytical model is beneficial for the feedback compensator design of an LLC resonant converter.

ACKNOWLEDGMENT

This work was supported by the National Science Council of Taiwan, Republic of China, under grant contract NSC 100-2221-E-214-006.

REFERENCES

- [1] E. X. Yang, F. C. Lee, and M. M. Jovanovic, "Small-signal modeling of series and parallel resonant converters," Proc. IEEE Applied Power Electronics Conference and Exposition, (APEC 92), Feb. 1992, pp. 785-792, doi: 10.1109/APEC.1992.228333.
- [2] A. K. S. Bhat, "Analysis and design of a series-parallel resonant converter," IEEE Transactions on Power Electronics, vol. 8, issue 1, 1993, pp. 1-11, doi: 10.1109/63.208493.
- [3] E. X. Yang, F. C. Lee, and M. M. Jovanovic, "Small-signal modeling of LLC resonant converter," Proc. IEEE Power Electronics Specialist Conference (PESC 92), Jun. 1992, pp. 941-948, doi: 10.1109/PESC.1992.254782.
- [4] B. Yang, "Topology investigation for front end DC/DC power conversion for distributed power system," Ph. D. Dissertation, 2003.
- [5] R. D. Middlebrook and S. Cuk, "A general unified approach to modeling switching converter power stages," Proc. IEEE Power Electronics Specialist Conference (PESC 76), 1976, pp. 18-34.
- [6] V. Vorperian and S. Cuk, "Small-signal analysis of resonant converters," Proc. IEEE Power Electronics Specialist Conference (PESC 83), 1983, pp. 269-282.
- [7] E. X. Yang, "Extended describing function method for small-signal modeling of resonant and multi-resonant converters," Ph. D. Dissertation, 1994.

APPENDIX

A. Parameters of Steady-State Solution

$$\begin{aligned} V_e &= \frac{4}{\pi} \cdot \sin(\pi \cdot d) \cdot V_g, & R_i &= 8n^2 R_L / \pi^2 = \frac{1}{R_e}, & I_{1s} &= \frac{\beta(1 + R_e \beta)}{\alpha^2 + \beta^2} V_e, \\ I_{1c} &= \frac{\alpha(1 + R_e \beta)}{\alpha^2 + \beta^2} V_e, & I_{2s} &= \frac{V_e}{\alpha^2 + \beta^2} \cdot (\beta + \frac{\alpha\beta}{L_m \Omega_s}), & I_{2c} &= -\frac{V_e}{\alpha^2 + \beta^2} \cdot (\alpha + \frac{-\beta^2}{L_m \Omega_s}), \\ V_{1s} &= \frac{\alpha(1 + R_e \beta)}{\alpha^2 + \beta^2} V_e \frac{1}{C_r \Omega_s}, & V_{1c} &= -\frac{\beta(1 + R_e \beta)}{\alpha^2 + \beta^2} V_e \frac{1}{C_r \Omega_s}, & \beta &= R_e (\Omega_s L_m)^2, \\ I_p &= \sqrt{(I_{1s} - I_{2s})^2 + (I_{1c} - I_{2c})^2}, & \alpha &= \left(\frac{1}{\Omega_s C_r} - \Omega_s L_r \right) (1 + R_e^2 \Omega_s^2 L_m^2) - \Omega_s L_m. \end{aligned}$$

B. Parameters of the Equivalent Circuit Model

$$\begin{aligned} E_{1s} &= \omega_0 L_r I_{1c}, & E_{2s} &= \omega_0 L_m I_{2c}, & E_{1c} &= \omega_0 L_r I_{1s}, & E_{2c} &= \omega_0 L_m I_{2s}, \\ K_s &= \frac{2(I_{1s} - I_{2s})}{\pi \cdot I_p}, & K_c &= \frac{2(I_{1c} - I_{2c})}{\pi \cdot I_p}, & g_{ps} &= g_{pc} = \frac{\alpha\beta}{R_e(\alpha^2 + \beta^2)}, \\ g_{pis} &= \frac{R_e \beta^2 \left(\frac{1}{C_r \Omega_s} - L_r \Omega_s \right)}{\alpha^2 + \beta^2}, & g_{pic} &= \frac{\beta \left(L_m \Omega_s - \frac{1}{C_r \Omega_s} + L_r \Omega_s \right)^2}{(\alpha^2 + \beta^2)}. \end{aligned}$$